

An Experimental Study on Angled Injection and Droplet Size Characteristics of Liquid Jets in Subsonic Crossflow

Min-Ki Kim*, Jinkwan Song*, Jeongjae Hwang*, Youngbin Yoon*
*School of Mechanical and Aerospace Engineering, Seoul National University,
San 56-1 Shinlim-dong, Kwanak-gu, Seoul, Korea, 151-742
ybyoon@snu.ac.kr

Keywords: Transverse Injection, Cavitation, Hydraulic flip effect, SMD(Sauter Mean Diameter), PLLIF(Planar Liquid Laser Induced Fluorescence), Angled Injection

Abstract

The spray characteristics and drop size measurements have been experimentally studied in liquid jets injected into subsonic crossflow. With water as fuel injection velocity, injection angle and atomizer internal flows were varied to provide of jet operation conditions. The injector internal flow was classified as three modes such as a non-cavitation flow, cavitation, and hydraulic flip flows.

Pulsed Shadowgraph Photography measurement was used to determine the spatial distribution of the spray droplet diameter in a subsonic crossflow of air. And this study also obtains the SMD(Sauter Mean Diameters) distribution by using PLLIF(Planar Liquid Laser Induced Fluorescence) technique.

The objectives of this research are getting a droplet distribution and drop size measurement of each condition and compare with the other flows effect. As the result, This research have been showed the droplet size were spatially dependent on air-stream velocity, fuel injection velocity, injection angle effects and normalized distance from the injector exit length.(x/d , y/d) There are also different droplet size characteristics between cavitation, hydraulic flip and the non-cavitation flows.

Introduction

The liquid fuel jets of perpendicularly injected into a subsonic crossflows has been studied for application in liquid-fueled high speed air breathing engines such as gas turbine engines, ramjet, scramjet engines and the after burner of gas turbine engines. Also, this transverse injection system is widely used in injection control device for highly combustion efficiency of aircraft engines. And the secondary fueled injection for reduced combustion instabilities. It is well known that the liquid fuel jet structure can be consist of three regimes: liquid column region, ligament region and the droplet region¹⁾. Generally, The jets also begins to bend in the direction of the crossflows. In the second phase, acceleration waves caused by the liquid column instability of the jet may undergo surface breakup²⁾. And, when amplified by the air flow, shed into ligaments. This is initiation of the third phase that rapidly collapses to form small droplets. And the liquid jet cross section changes from circular to kidney-shaped as the jet exits the orifice into the crossflows. In this way, this breakup mechanism and droplet characteristics is very important parameters

for designing an injector and a combustor to optimize combustion efficiency. There are many kind of experimental and mathematical modeling studies in liquid column trajectory and mixing rate of transverse jets. Adelberg et al.³⁾ analytically predicted the mean drop size generated by a liquid jet penetrating a high-speed gas stream($We \cdot Re > 10^6$). Ingebo et al.⁴⁾ They measured the acceleration waves in liquid column surface by aerodynamic drag force at $We \cdot Re < 10^6$ using the scanning radio meter technique. Although the previous studies showed visually that droplet sizes were spatially dependent, quantitative results were available only for a spatially averaged droplet size correlation. Kihm et al.⁵⁾ were correlation of drop Sauter Mean Diameter normalized to the orifice diameter was obtained from all the experimental data. For example penetration length and air, fuel velocities by the Malvern System. Wu et al.⁶⁾ found that SMD distribution in droplet region by PDPA method. And Sankar et al.⁷⁾ suggest that Sauter Mean Diameter can be directly measured by ratio the intensities of laser-induced fluorescence and elastic light scattering from spray field. Tamaki et al.⁸⁾ found that cavitation and hydraulic flip effects were very important factor for breakup process in liquid jets. Therefore, we have studied effects of the cavitation and hydraulic flip on perpendicular injection system, especially spray plume structures and SMD distribution using the Planar Liquid Laser Induced Fluorescence(PLLIF) and Direct Photography experimental technique. And to understand the droplet size characteristics of injection angled effects into the crossflows.

Experimental Apparatus and Conditions

Design of injectors

The orifice diameter of injectors was 0.5mm. The injector inside consist of internal chamber and an orifice. The internal chamber size is 12mm. So, these orifices have a chamber-to-orifice diameter ratio of 24. For testing non-cavitation and cavitation flows, round-edged and sharp-edged orifices shape were designed, as shown in Fig.1 (a), (b) and (c). The sharp-edged orifices are used for metering flows in different applications. According to previous works has shown that an orifice can be considered to have a sharp-edged entry when its entry radius is less than about 0.14 times the diameter of the orifice. There are no happened vena-contracta form. In order to obtain the non-cavitation flows, round-edged orifice were used

with a curvature radius of one diameter of the orifice which have a length-to-diameter ratio of 20. On the other hand, sharp-edged orifices were designed to obtain cavitation and hydraulic flip effects. For obtain the hydraulic flip flows, we made a length-to-diameter ratio of 5 orifices caused by generally previous work has reported that if length-to-diameter ratio was less than about 8. It takes hydraulic flip flows. Lastly, in order to obtain the droplet size characteristics and liquid column trajectory injection angled effects, the angled injector were designed as shown in Fig.1 (d) such as the orifice injection angle is 30, 60, 90, 120, 135, 150 degrees.

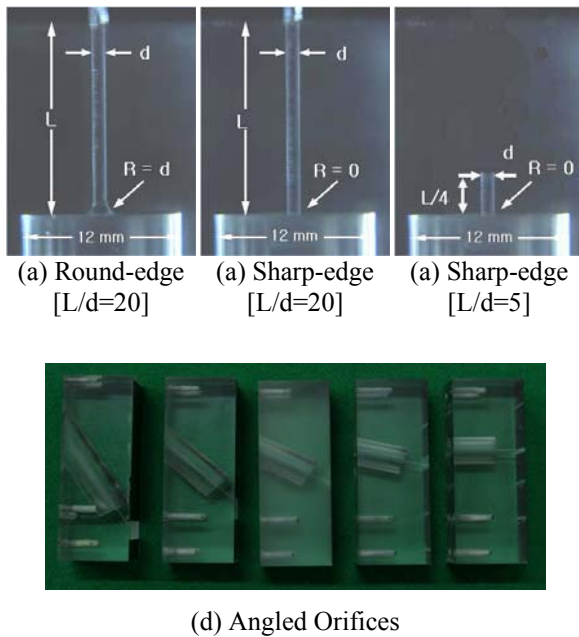


Fig. 1 Experimental apparatus

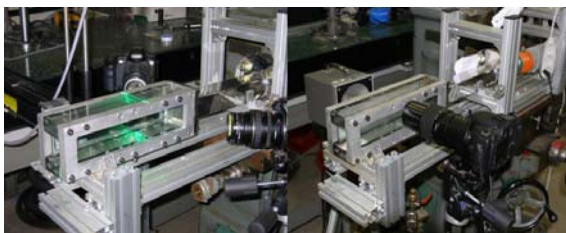


Fig. 2 Experimental Setup for PLLIF and Direct Photograph Technique

Experimental condition and method

First of all, we measured mass flow rate of non-cavitation, cavitation and hydraulic flip flows by using direct mass flow measurement. The liquid jets ejecting from the orifice exit were visualized using the digital stroboscope with a pulse duration of approximately 600rpm, which could freeze the motion of the liquid column and droplets and were recorded on a digital camera(Canon EOS 20D). For the accurately measurement of droplet size and liquid column trajectory, we used the highly magnification single optical lens as Canon MP-E 65mm f/2.8 1-5X Macro Photo. Table 1. shows the injection angle dimensions of orifice design parameter and experimental

conditions. We can measure the droplet images of 3000 to 4000. At this time, the magnification of this experimental equipment is 2 micron meter per one pixel with accuracy ranges at nearly below the 5%⁹⁾. Fig. 2 shows the configuration of the Planar Liquid Laser Induced Fluorescence and Direct Photography experiment used in this research work. As shown in this figure, the wind tunnel has a rectangular cross section of 50 X 50 mm and a length of 330mm with visualization acrylic windows. For the Planar Liquid Laser Induced Fluorescence measurement technique, we used continuous beam of Ar-ion laser(Spectra-Physics, Model 2020) was spread as a sheet beam by a fiber-optics(Dantec). The mixture of water and ethyl alcohol(of volumetric ratio 4:1) was used as simulants of fuel, and fluorescein (C₂₀H₁₂O₅, Aldrich F245-6) of 30mg was dissolved into the simulant of 1liter. Because of the fluorescein absorbs light in the wavelength range from 400 to 530nm with the peak wavelength at about 488nm the Ar-ion laser beam of 488nm in wavelength was used. The emission spectrum of the fluorescein in the present simulant was measured using a monochromator, and it was found that the spectrum ranged from 500 to 650nm and that the peak emission appears at 525nm. After being separated from the scattering signal by an high-pass filter that cuts off wavelengths below 550nm, the fluorescence signal was recorded on a digital camera (Canon 20D, 12-bit, 3504×2336). Likewise, the mie-scattering images getting by 514±5nm band-pass filter.

Table 1. Experimental conditions

parameter	value
Air velocity	60±1 m/s
Air Temperature	300 K
Fuel Temperature	318K (45°C)
Fuel	Water : Ethanol = 4 : 1
Orifice Diameter	0.5 mm
Orifice Shapes	Round edged (L/d=20), Sharp edged (L/d = 5, 20)
ΔP(bar)	1,2,3,4,5,6
x/d	40, 60, 80, 100, 120
Injection angle	30°, 60°, 90°, 120°, 135°, 150°

Results and Discussion

Flow Characteristics of Internal Conditions

We measured the mass flow rates of each internal flows condition such as the non-cavitation, cavitation and hydraulic flip flows. First of all, we used the boiling water for cavitation flow effect. And this working fluid contains the fluorescein for flow

visualization. Fig. 3 shows the discharge coefficients for round-edged and sharp-edged orifices as a function of pressure differential (1 to 6 bar) where the theoretical equation of discharge coefficient under cold and hot flow conditions as follow;

$$C_d = \frac{\dot{m}}{A\sqrt{\rho_f \Delta P}} \quad (1)$$

As the discharge coefficient increases, the pressure differential increases all of orifices shape before cavitation effect occurs. The discharge coefficient of round-edged orifice is higher than those of sharp-edged orifices caused by the orifice internal flows effect. Shows the round-edged orifices in the Fig. 3 graph the discharge coefficient increases slightly as the injection pressure increases respectively.

As the sharp-edged orifices with length-to-diameter ratio of 20, the discharge coefficients were decreases gradually after 3.5bar caused by cavitation effect but before the pressure differential of 3.5bar, the discharge coefficients increases gradually like the non-cavitation flow effect with round-edged orifice. On the other hand the discharge coefficient of sharp-edged orifices with a length-to-diameter ratio of 5.

There are two kind of flows effect occur. One is the gradual drop in the hydraulic flip region and the other is sudden drop in the cavitation region, as shown Fig. 3. After the sudden drop in the range of pressure differential 3bar to 6bar, the discharge coefficient remains at almost same value due to the surface of liquid flow is detached from the inner wall of the injector exit hole. So, the liquid column size is smaller than the non-cavitation and cavitation flows condition. And the mass flow rate also small at the same condition.

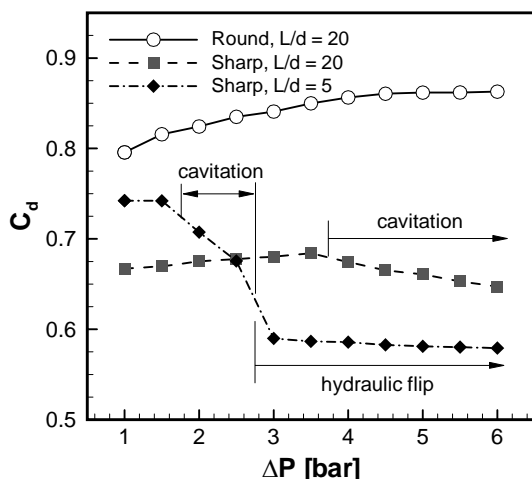


Fig. 3 Discharge Coefficients of each injection pressure difference

SMD Distributions through the PLLIF Technique

According to the Lorenz-Mie theory, the scattered intensity of the spherical droplet at an arbitrary position depends on various parameters such as the

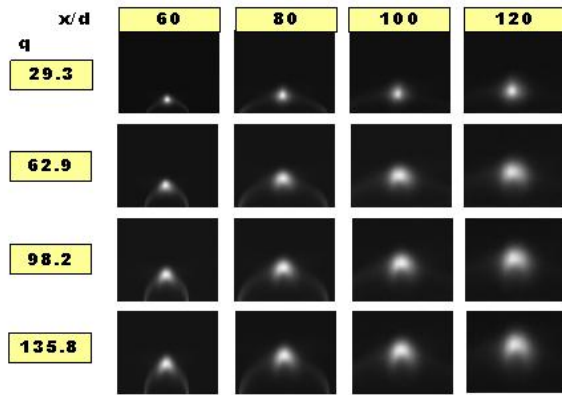
diameter and the refractive index of droplets, the polarization and the wavelength of the incident light, and so on. In 1999 Sankar et al. ⁷⁾ however, have found that for weak absorbing droplets the scattered light intensity can be treated to be proportional to the square of the droplet diameter by calculations based on the Lorenz-Mie theory. It is well known that the fluorescent signal is dependent on the concentration of fluorescing molecules, for low laser light absorption conditions. Thus, the fluorescence signal intensity from a droplet is proportional to the cube of its diameter, if it is a sphere. In other words, the fluorescent signal intensity is proportional to the volume of droplet, i.e. to the mass of droplet when the fluorescing materials are distributed uniformly in the test fluid and do not vary in composition which is typical for evaporating droplets. The mie scattered signal intensity from a droplet is proportional to the square of droplet diameter.

$$\frac{G_f(x,y)}{G_s(x,y)} = \frac{c_f}{c_s} \left[\frac{\sum N_i(x,y) d_i^3(x,y)}{\sum N_i(x,y) d_i^2(x,y)} \right] \quad (2)$$

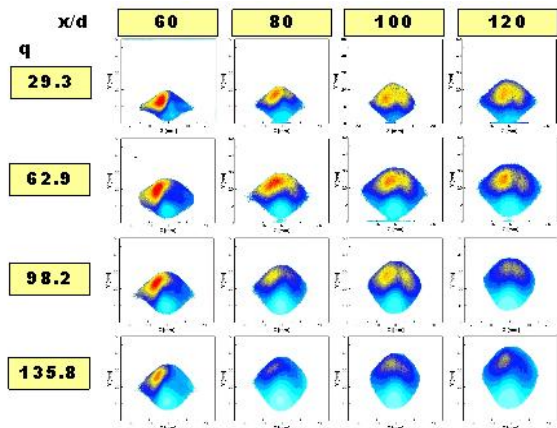
$$D_{32}(x,y) = \frac{1}{K} \left[\frac{G_f(x,y)}{G_s(x,y)} \right] \quad (3)$$

Equation (3) shows that the measured fluorescent intensity and the scattered intensity can be directly used to compute the SMD if appropriate constant K is defined. We measured the constant K exactly from the direct photograph technique with high magnification images. Likewise, to measure the droplet size distribution of the spray with planar imaging technique, it is necessary to obtain both images of the fluorescence and Mie-scattering by incident laser light simultaneously. Fig. 4 presents cross-sectional images of fluorescein and SMD profiles when the spray injection angle 90 degree and the pressure differential of 4 bar during the non-cavitation flow. At the same normalized x-axis distance, as pressure difference that is fuel/air momentum flux ratios increase, penetration increases and the spray distribution becomes more broader and vortex structure becomes more apparent. However, the width does not have a noticeable change. In the same pressure differential, normalized x-axis increases as penetration also increases and the spray distribution becomes broader. And we can explain as the liquid/air momentum flux ratio, q is increased to 135.8, the outer spray shape becomes more elliptical although the inner rings of the spray exhibit slight indentations at the rear. The indentations in the inner rings are more pronounced here and imparts a distinct vortex pair-induced kidney shape typically found in jet interaction with a crossflow. The kidney shape spray form is caused by counter-rotating vortex pair. This shape is well known fact through the many previous researcher results. If the fuel/air momentum flux ratios increase as liquid jet penetration increases however, SMD was getting smaller. And the normalized x-axis

distance increase as SMD was decrease because of secondary breakup by aerodynamic forces. As you can see, there are many kind of very small size droplets diameter existence. Such as below the $50 \mu\text{m}$.



(a) Fluorescein Images



(b) SMD profiles in the Cross-section

Fig. 4 Cross-Sectional distributions of SMD and LIF images at non-cavitation flow, $\Delta P=4\text{bar}$, 90° injection

Droplet Size Characteristics

We take the high magnification droplets which is non-cavitation, cavitation and hydraulic flip flow condition from the direct photography technique. Fig. 5 shows the spray patterns by various injection angled effects and the high magnification droplet images. And the SMD versus y for different injection pressure and normalized distance x/d at the non-cavitation flows are shown in Fig. 6. Likewise, our experimental conditions such as the $We \cdot Re$ values above 10^6 , the SMD was decrease caused by acceleration wave breakup effect. The liquid column ligaments are then atomized into droplets when the liquid surface is relatively flats, as in the case of fairly large orifice diameter, Adelberg et al.³⁾ predicts that a capillary wave type of breakup will occur. And the droplet size was decrease as the liquid penetration was increases by the injection pressure differential of orifice. So, aerodynamic force and surface breakup were increase as in that case. Also, larger droplets penetrate further away in the y -direction as x increases. Relatively

smaller droplets will then downstream along the same y -distance from the nozzle exit. It is believed that the SMD decrease is attributed to the depletion of larger droplets as x increases on the same y .

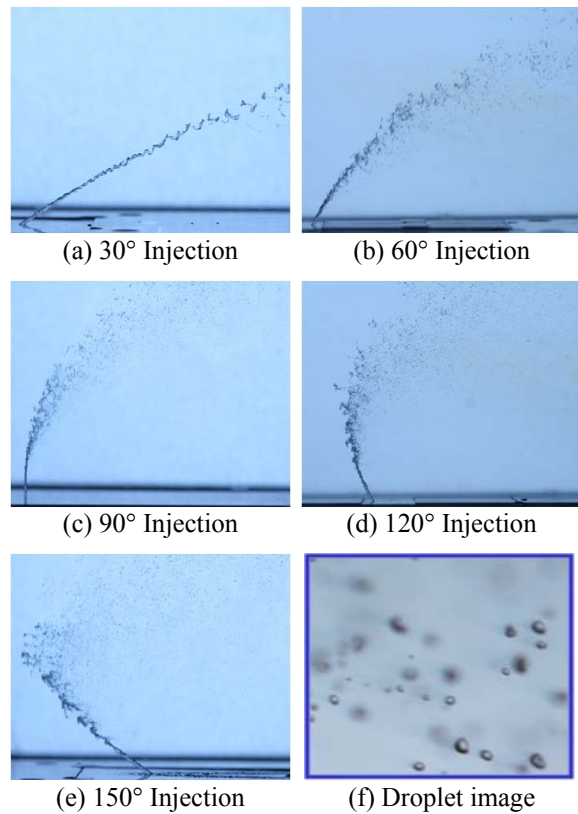


Fig. 5 Spray patterns by various injection angled effects and the high magnification droplet images

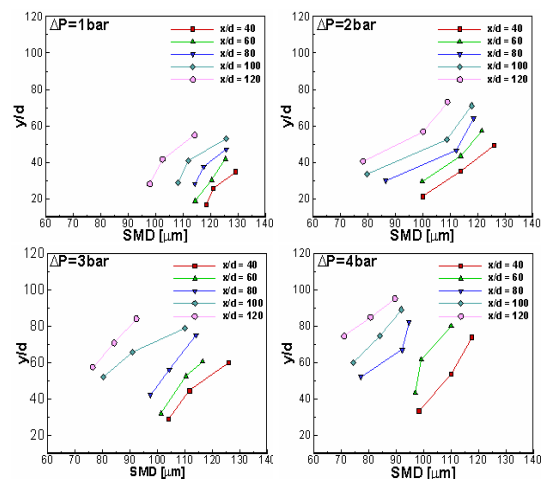


Fig. 6 SMD versus y for different injection pressure and normalized distance x/d at the non-cavitation flow

Fig. 7 graph indicated the effect of internal flow result by normalize transverse distance profile graph of SMD distribution. The injection velocity was fixed to 21m/sec and orifice diameter was also fixed to 0.5mm . It is well known result that the liquid jet penetrates the gas flow and atomization take place, larger drops tend to move out farther into the air

stream than smaller drops caused by the greater momentum of the larger drops. So, the mean droplet size distributions will increase monotonically farther away from the injector orifice exit. When the cavitation effects occur, SMD of cavitation flow are smaller than those of non-cavitation flow because of liquid jet become more turbulent and unsteady. On the other hand, when hydraulic flip effects occur, SMD of hydraulic flip flow are smaller than those of the other flows effect because of liquid column jet diameter of hydraulic flip flow is smaller than that of other flows effect as same working conditions.

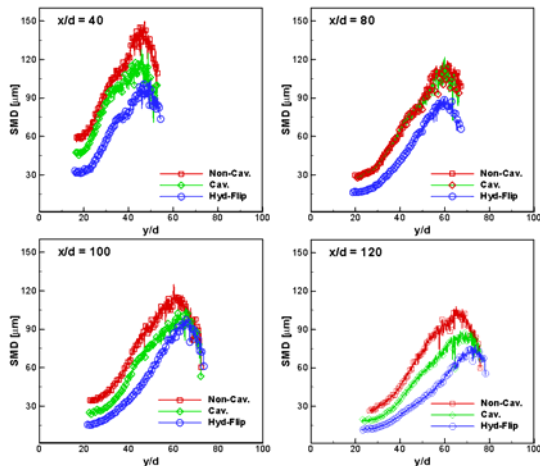


Fig. 7 SMD distributions along the X-axis under non-cavitation, cavitation, and hydraulic flip flows ($v_f = 21.05$ m/s, $d = 0.5$ mm)

The injection parameter ratios of non-cavitation, cavitation and hydraulic flip flows are summarized in the table 2. They are normalized by parameters of non-cavitation flow. When cavitation effect takes place, the mass flow rate decreases to about 75%. But liquid jet area of orifice exit doesn't decrease. So, jet velocity of cavitation is about three-quarter times as fast as that of non-cavitation flow. On the other hands, in case of hydraulic flip flow, mass flow rate decreases to about 66% and liquid jet area of orifice exit also decreases to 77%. Hence, Jet velocity is 0.86 times as fast as that of non-cavitation flow; it is more faster than jet velocity of cavitation flow. As a result, the droplet size of cavitation and hydraulic flip flows effect are smaller than non-cavitation effect flow field.

Table 2. Parameter Ratios

parameter	Non-cavi.	cavitation	Hyd-flip.
$\frac{(\dot{m})_{effect}}{\dot{m}}$	1	0.75~0.8	0.66
$\frac{(\dot{A})_{effect}}{\dot{A}}$	1	1	0.77
$\frac{(\dot{v})_{effect}}{\dot{v}}$	1	0.75~0.8	0.86

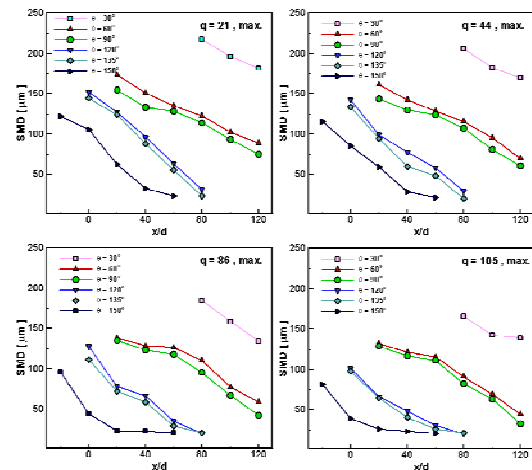


Fig. 8 SMD results of each injection angled effect using a direct photography technique

Measurements are carried various different x-distances and injection angled of the nozzle to inspect the spray development along the air flow direction. Fig. 8 presents the results in terms of Sauter Mean Diameter(SMD) versus normalized transverse distance for the case of various injection angled effects through a 0.5mm injector. Preferential evaporation of smaller droplets also contributes to an increasing SMD along the spray axis. A decrease in SMD along with the air flow is observed in the present case of cross injecting atomization. The mean droplets size is also small which spray injection angle is decreased. If the spray injection angle is 30 degree such as, the normal injection crossflow air stream, there are some non-aerodynamic effect existence. And the reversed injection air-stream flow such as above the 90 degree. The droplets diameter is very smaller than normal injection condition caused by aero dynamic effect. We can know that the SMD is function of varied injection parameters for example Weber, Renolds number, orifice diameter, injection angle, axial and penetration distance etc. So, we will study of SMD empirical formula to the next research.

Conclusion

The liquid jet and atomization test in subsonic crossflow were carried out to analyze droplets size characteristics of various injection parameter and orifice internal flows condition. Our results can be summarized as follows;

The Sauter Mean Diameter (SMD) decreases as one move downstream from the injector exit by the aerodynamic force. And the lager droplets tend to move out farther into the air stream than smaller droplets because of the greater momentum of the larger droplets. The largest droplets are formed in the middle and high of the jet plume by SMD profiles in the Cross-section. Like the preceding, the droplet diameter decreases as the dynamic pressure ratio q increases and vice versa, a decrease in surface tension at lower dynamic pressure ratio q decreases the droplet diameter. Also, we can found that the SMD

can be directly measured by ratio the intensities of laser-induced fluorescence and elastic light scattering from the spray. In case of cavitation and hydraulic flip flows, overall SMD are smaller than non-cavitation flow because of the liquid jet to become turbulent, unsteady and the mass flow rate was decreases from hydraulic flip flow condition. About the Injection angled effects, the SMD was decreases as injection angle θ was increases such as the reversed injection at the same working conditions. So, we can conclude that the droplet sizes dependent on liquid fuel velocity, axial, penetration distances and each internal flows effect.

Acknowledgement

This work has been supported by Ministry of Science and Technology Grants 0498-20070011, contracted through the Interdisciplinary Research and the Institute of Advanced Aerospace Technology at Seoul National University.

Nomenclature

A	orifice area
c, C	constants
C_c	cavitation coefficient
C_d	discharge coefficient
d	orifice diameter
L	orifice length
\dot{m}	liquid mass flow rate
P_1	total pressure in the pressure vessel
P_2	ambient pressure
P_v	vapor pressure
q	liquid/air momentum flux ratio, $\rho_f u_f^2 / \rho_g u_g^2$
u_f	liquid velocity at the orifice exit
u_g	gas velocity in the airstream direction
x	distance in the airstream direction
y	distance in the direction transverse to the airstream
y_t	top height of spray distribution
y_m	maximum mass flow rate height of spray distribution
y_b	bottom height of spray distribution
z_w	width of spray distribution

Greek

ρ_f, ρ_l	liquid fuel density
ρ_g	gas density in the test section
ΔP	injection pressure differential

subscript

cav	cavitation
eff	effective value
f, l	liquid property
g	gas property
non	non-cavitation
hyd	hydraulic flip

References

- 1) Schetz, J.A. and Padhye, A., "Penetration and Breakup of Liquids in Subsonic Airstreams", AIAA Journal, 15, 1385-1390, 1977.
- 2) Fric, T.F. & Roshko, A. "Vortical structure in the wake of a transverse jet.", J. Fluid Mech. 279, 1-47., 1994. *Power*, 11 (1), 1995, pp. 135-145.
- 3) Adelberg, M., "Mean Drop Size Resulting from the Injection of a Liquid Jet into a High-speed Gas Stream", AIAA J., vol. 6, no. 6, June 1968, pp. 1143-1147.
- 4) Ingebo, R. D., "Effect of Airstream Velocity on Mean Drop Diameters of Water Sprays Produced by Pressure and Air Atomizing Nozzles", NASA TM-73740, 1977.
- 5) K. D. Kihm, G.M. Lyn, S.Y. Son, "Atomization of Cross-Injecting Sprays into Convective Air Stream", Atomization and Spray, vol. 5, pp. 417-433, 1995.
- 6) Wu, P. K., Kirkendall, K. A., Fuller, R. P., and Najad, A. S., "Spray Structures of Liquid Jets Atomized in Subsonic Crossflows," Journal of Propulsion and Power, Vol.14, No.2, pp.173-182, 1998.
- 7) S. V. Sankar, K. E. Maher, D. M. Robert, W. D. Bachalo "Spray Characterization Using a Planar Droplet Sizing Technique," ICLASS-97, August 18-22, 1997, Seoul.
- 8) Tamaki, N, Shimizu, M, Nishida, K, and Hiroyasu, H, "Effects of Cavitation and Internal Flow on Atomization of a Liquid Jet," Atomization and Sprays, Vol.8, pp.179-197, 1998.
- 9) Lefebvre, A. H., Atomization and Sprays, Hemisphere Publishing Corp. Philadelphia, 1989.
- 10) K. Ahn, J. Kim, Y. Yoon, "Effects of Orifice Internal Flow on Transverse Injection into Subsonic Crossflows: Cavitation and Hydraulic Flip," Atomization and Sprays, Vol.16, No.1, 2006.